DOI: 10.3969/j.issn.1673-3185.2017.05.014 **http**: // english.ship-research.com

Translated from: CEN Z L, LIU T, WANG L, et al. Leakage analysis of fuel gas pipe in large LNG carrier engine room[J]. Chinese Journal of Ship Research, 2017, 12(5): 109-119.

Leakage analysis of fuel gas pipe in large LNG carrier engine room

CEN Zhuolun, LIU Tao, WANG Lei, DOU Xu

R&D Dept., Hudong-Zhonghua Shipbuilding (Group) Co., Ltd., Shanghai 200129, China

Abstract: [Objectives] The electric propulsion dual-fuel engine is becoming dominant in newly built Liquefied Natural Gas (LNG) carriers. To avoid the potential risks that accompany the use of flammable and explosive boil-off gas, the performance of precise safety and reliability assessments is indispensable. **[Methods]** This research concerns the engine rooms of large LNG carriers which are propelled electrically by a dual-fuel engine. Possible fuel gas (natural gas) leak cases in different areas of the engine room are simulated and analyzed. Five representative leak cases defined by leak form, leak location and leak rate are entered into a Computational Fluid Dynamics (CFD) simulation, in which the Reynolds stress model of Fluent software is adopted as the turbulence model. The results of the leaked gas distribution and ventilation velocity field are analyzed in combination to obtain the diffusion tendency and concentration distribution of leaked gas in different areas. **[Results]** Based on an analysis of the results, an optimized arrangement of flammable gas detectors is provided for the engine room, and the adoption of an explosion-proof exhaust fan is proven to be unnecessary. **[Conclusions]** These analysis methods can provide a reference for similar gas leakage scenarios occurring in confined ventilated spaces. In addition, the simulation results can be used to quantitatively assess potential fire or explosion damage in order to guide the design of structural reinforcements.

Key words: Liquefied Natural Gas (LNG) ; pipe leakage; Computational Fluid Dynamics (CFD) ; quantitative risk assessment

CLC number: U664.14

0 Introduction

With the improvement of environmental protection regulations and emission standards, ships with clean gases such as Liquefied Natural Gas (LNG) as power fuel have been developed rapidly[1-3]. LNG will become the dominant fuel for the future shipping because of its cost advantage and the continuous improvement of its supporting infrastructure by developed countries[4-7]. However, natural gas leakage may occur due to fatigue damage caused by bad sealing of fittings of natural gas pipe, pipeline vibration and alternation of cooling and heating, or sour corrosion of high-sulfur fuel, and even unforeseeable factors such as man-made operation. Natural gas is colorless and tasteless, and thus leakage is difficultly perceived. Burning explosion may occur if natural gas meets spark after long-time accumulation[8-9]. When the molar concentration of natural gas is greater than 4.9%, burning explosion may happen (calculation by pure methane). Besides, overhigh concentration may also stifle people. Therefore, it is necessary to accurately assess and effectively avoid the application risk of natural gas.

In terms of quantitative calculation for field distribution of gas flow diffusion, Computational Fluid Dynamics (CFD) can simulate physical effects such as natural flow, thermodynamic motion of mixture, and molecular diffusion caused by compressibility, turbulent flow, and density difference of fluid, and it applies to simulation verification for diffusion process of gas with complex turbulent flow[10-11], and risk assessment for leakage and diffusion of flammable and explosive gases.

Received: 2017-03-14

Author(s): CEN Zhuolun (Corresponding author), male, born in 1988, master, engineer. Research interest: development and design of LNG low-temperature liquid cargo disposal system. E-mail: cenzhuolun@hotmail.com

LIU Tao, male, born in 1983, Ph.D., senior engineer. Research interest: development and design of marine system. E-mail: smuliutao@163.com

DNV (2006)[12] adopted FLACS and KFX software to assess the leakage and burning explosion risks of high-pressure fuel-gas supply system (from MAN Company) of a certain engine in engine room. Cheng et al. (2011)[13] conducted CFD analysis for diffusion and leakage of natural gas pipe under different wind conditions in confined spaces of urban streets. Wang (2014)[14] analyzed the effects of wind velocity, wind direction, and leakage direction on the leakage and diffusion of oil and gas in ocean platform by using Fluent software. Fu et al. (2016)[15], with the combination of event tree analysis and CFD analysis, investigated the occurrence probability of leakage accidents in LNG carrier, and quantitatively evaluated the severity of leakage accidents. In the same year, Fiates et al.[16] simulated and analyzed the leakage and diffusion of methane and carbon dioxide in ocean platform and wind tunnel by using OpenFOAM software. IMO[17] assessed the potential risks in LNG fuel pretreatment room of a large ore carrier by event tree analysis and fault tree analysis, and performed quantitative evaluation on burning explosion accident consequences by CFD method. However, few studies focus on simulation calculation of leakage accidents to guide prevention mechanism (such as arrangement of flammable gas detectors) and explosion-proof design of equipment.

This paper performs simulation calculation for leakage accidents in engine room of a new LNG carrier (1.74×10^5 m^3), the arrangement of flammable gas detectors, and the demand evaluation of explosion-proof exhaust fan. Leakage and burning explosion risks of fuel gas exist in the engine room which is the core power unit, and the possibility and severity of burning explosion are closely related with leakage amount and concentration of fuel gas. Therefore, commercial CFD software Fluent is used for calculating and analyzing gas flow in the engine room as well as leakage and diffusion of fuel gas: firstly, the characteristics of ventilation flow field is analyzed, and the fuel gas pipes are separated according to different areas of the engine room; then, the representative leak points are selected in different areas, and the diffusion tendency and concentration distribution of leaked natural gas cloud (hereinafter referred to as "gas cloud") are calculated; finally, flammable gas detectors are properly arranged to reduce the burning explosion risk to the utmost extent.

1 Modeling and calculation

1.1 Calculation method

The unsteady Reynolds averaged Navier-Stokes (N-S) equation is used for calculation of air flow in the engine room, and component transport equation is applied to calculating the diffusion flow of leaked natural gas. In *xyz* rectangular coordinate system, control equation is shown below after time-averaged treatment[18-19]:

$$\frac{\partial \Phi}{\partial t}+\operatorname{div}(\Phi \boldsymbol{U})=\operatorname{div}\left(\Gamma_{\Phi}^{*}\operatorname{grad}\Phi\right)-\left(\frac{\partial \overline{u'\Phi'}}{\partial x}+\frac{\partial \overline{v'\Phi'}}{\partial y}+\frac{\partial \overline{w'\Phi'}}{\partial z}\right)+S_{\Phi} \qquad (1)$$

where Φ and Φ' are respectively time-averaged variable and corresponding pulsating quantity of fluid; t is time; $\boldsymbol{U}$ is time-averaged velocity vector, including 3 velocity components (u, v, w) in three directions of rectangular coordinate system; u', v', w' are corresponding pulsating quantities of u, v, w; Γ_{Φ}^{*} is a generalized diffusion coefficient; S_{Φ} is a generalized source item.

There are 21 air inlets of different dimensions in the ventilation system of the engine room. By taking intake air as jet flow, different incident velocities of intake wind may cause extensive mixing and momentum exchange in flow field, and meanwhile, large-area trailing vortex will be formed in the leeward sides of different shapes of large equipment and structural platforms in the engine room. There is abundant shear flow in the whole engine room, and thus, Reynolds Stress Model (RSM) is selected as the turbulence model to close the Reynolds stress item in the N-S momentum equation during calculation. Compared with k-ε turbulence models of the two equations, RSM directly establishes six transport equations for Reynolds stress components, plus a dissipation equation for calculation[19], and abandons the two assumptions of strain with Reynolds stress in direct proportion to time-averaged velocity and isotropous turbulent viscosity to calculate turbulence stress.

RSM is widely applied to predicting the diffusion process of unsteady turbulent flow in confined spaces. Cehlin et al.[20] investigated the effect of gas distributors on air flow in a room, and the steady simulation result of air velocity distribution obtained by RSM was consistent with the test result; besides, they pointed out that the result of unsteady simulation would be more accurate. Guo et al.[21] adopted RNG k-ε model and RSM to calculate the effect of buildings on the diffusion of contaminants, and they found that RSM has a better effect in predicting the concentration distribution of contaminants and changes of surrounding flow field. Therefore, in this paper, RSM is taken as the turbulence model, and the boundary conditions similar to References [20] and [21] are set; then, unsteady simulation calculation is conducted for leakage and diffusion of fuel gas in well-ventilated engine room.

1.2 Modeling of the engine room

1.2.1 Fuel-gas supply system and flammable gas detection system

The diagram of fuel-gas supply system in the engine room is shown in Fig. 1. The prime motor is arranged in the engine room, and MAN DIESEL dual-fuel medium-speed engine is used by taking volatile gas as fuel in LNG cargo tank during navigation.

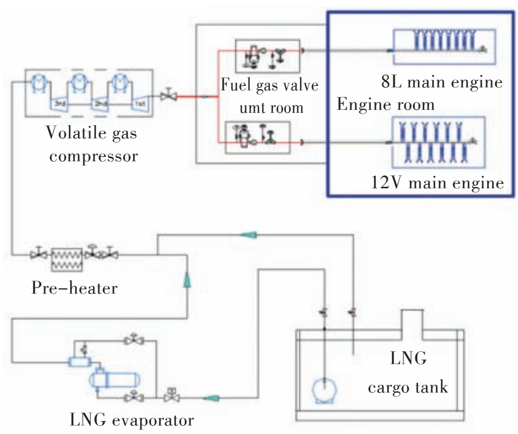

Fig.1 Fuel-gas supply system diagram

In the engine room as the core unit of power system, besides engine unit, there are a delivery pump, a fan, a travelling crane and other electrical equipment, whose violent vibration will increase the leakage and burning explosion risks of fuel gas. Once leakage happens, the last safety curtain is that external flammable gas detectors effectively feedback and start up the cut-off mechanism in time. This carrier adopts stationary flammable gas detectors. When any sensor reaches 20% of the lowest explosive limit, it will give an alarm and start the prevention mechanism. Therefore, the proper arrangement of flammable gas detectors is the basis for the detection system to accurately give an alarm in advance, and the arrangement scheme shall be evaluated before installation. According to the traditional arrangement scheme, one detector is generally arranged at each corner (four corners in total) in the above space of the engine, as shown in Fig. 2.

1.2.2 Geometric modeling of the engine room

The three-dimensional model of the engine room is shown in Fig. 3. The room is about 22.4 m in longitudinal length, 20.65 m in transverse width, and 10.14 m in height. As shown in Fig. 3(a), one 12V

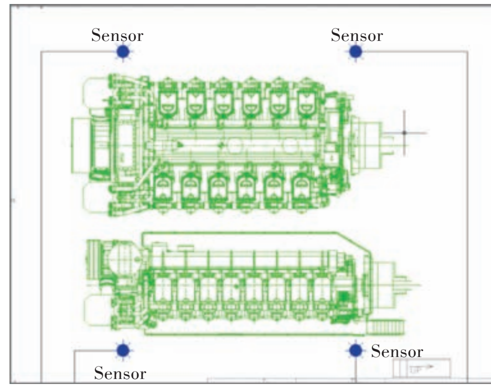

Fig.2 Traditional arrangement of flammable gas detectors for engine room

dual-fuel engine, one 8L dual-fuel engine, and three air ducts are arranged in the engine room, where there is a layer of structural platform in the middle. In Fig. 3(b), the area in the right back side of the room (starboard at stern) is sealed by ship-hull plate.

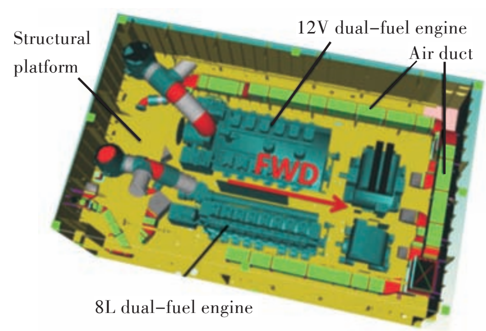

(a) Engine room

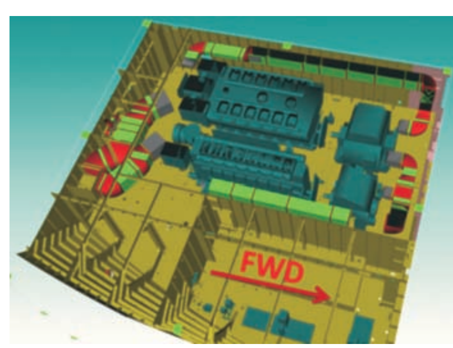

(b) Area in the right back side of engine room

Fig.3 Three-dimensional model of engine room

The area with arrangement of fuel gas pipes in the engine room is divided into three parts, as shown in Fig. 4.

CFD geometric model is established according to the three-dimensional model of engine room (Fig. 3), as shown in Fig. 5. This paper adopts uniform global coordinates: x axis is along the carrier length, with bow direction as the positive direction; y axis is along the carrier width direction, with larboard direc-

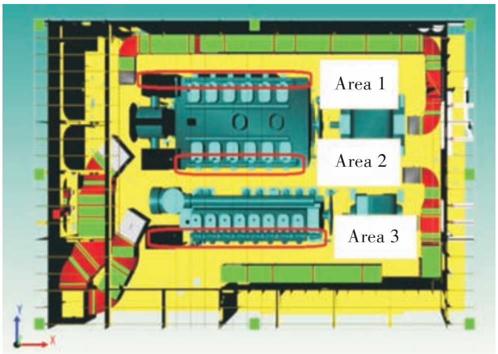

Fig.4 Divided partitions of fuel-gas supply pipeline in engine room

tion as the positive direction; z axis is along the carrier height direction, with upward direction as the positive direction.

1.3 Mesh division

The structured hexahedral meshes are used for the open space without barriers above the engine room, and the unstructured tetrahedral meshes are used for other areas, so as to improve the precision of geometric modeling on the surface. With comprehensive consideration of precision requirements and simulation time, the global mesh size is set to be 0.3 m. The meshes are densified at leakage sources and air inlet and outlet with large changes of physical parameters, as well as in the ventilation confluence area above the engine, while global settings are used away from the leakage sources and air inlet and outlet to reduce simulation time. The maximum Skewness of meshes is smaller than 0.85, and the maximum Skewness of above 90% of meshes is smaller than 0.6. The number of meshes is in the range of 6×10^5–1.20×10^6 (the number of meshes is different under different leak cases), and an example of meshing for the overall computational domain is shown in Fig. 6.

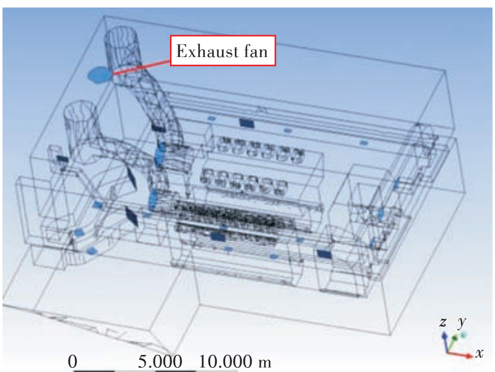

(a) Three-dimensional projection of engine room (blue signs are the boundaries of air inlet and outlet)

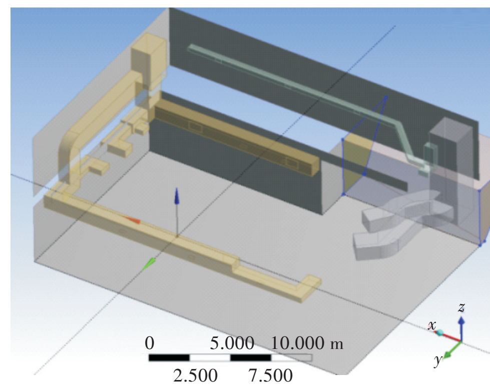

(b) Three-dimensional view of three air ducts (a part of bulkhead and all equipment are hidden)

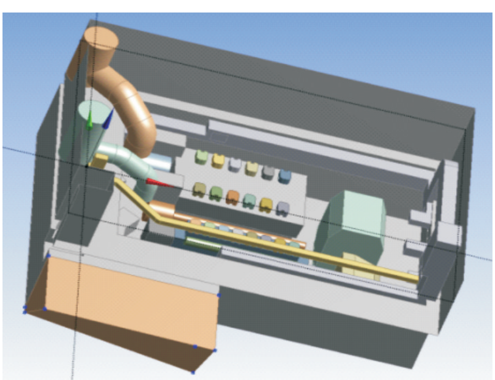

(c) Global three-dimensional view

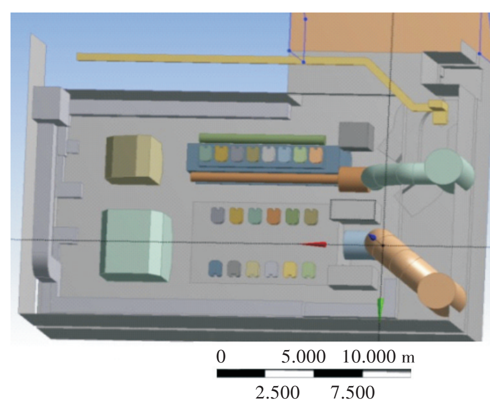

(d) Three-dimensional enlarged view (a part of bulkhead is hidden)

Fig.5 Geometry built for CFD analysis

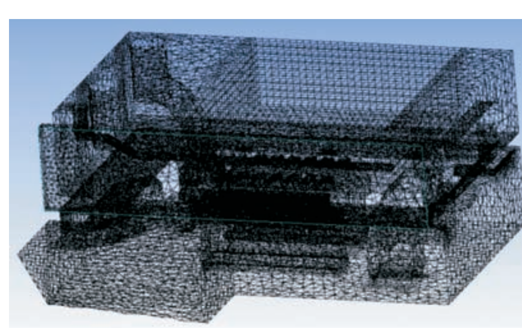

Fig.6 An example of meshing

1.4 Definition of leak cases

According to overall arrangement of engine room, the location of fuel gas pipe, simulation result of ventilation flow, and leak form, five leak cases are defined, as shown in Table 1.

Table1 Definition of leak cases

Leak case	Size of leak point/ mm	Flow rate at outlet/($m \cdot s^{-1}$)	Leak form	Location of leak point
Case 1	20×20	66.29	Continuous leak	Connection location of flexible hose of 8L engine
Case 2	20×20	66.29	Continuous leak	End of fuel gas pipe at the top of 8L engine
Case 3	20×20	66.29	Continuous leak	Connection location of flexible hose of 12V engine
Case 4	20×20	66.29	Continuous leak	End of fuel gas pipe at the top of 12V engine
Case 5	20×20	66.29	Continuous leak	Middle section of fuel gas pipe at the top of 12V engine

1.4.1 Location selection of leak points

Based on division areas of fuel gas pipe (Fig. 4), air flow tendency in engine room, and easy leakage location, five leak points are selected in three areas of fuel gas pipe, as shown in Fig. 7.

Because of equipment vibration and insecure connection, the connection location between fuel gas pipe and flexible hose of the engine may become the leak points more easily. Therefore, the connection locations of flexible hoses of 8L and 12V engines are selected as leak points 1 and 3, as shown in Figs. 7(a) and 7(b), i.e., Case 1 and Case 3. According to the ventilation flow field in the areas of fuel gas pipe, the ends of fuel gas pipe at the top of 8L and 12V engines are selected as leak points 2 and 4, as shown in Figs. 7(a) and 7(b), i.e., Case 2 and Case 4. The middle section of fuel gas pipe at the top of 12V engine is taken as leak point 5, as shown in Fig. 7(c), i.e., Case 5.

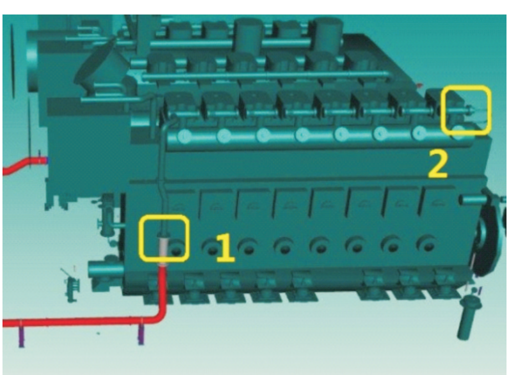

(a) Case 1 and Case 2 (leak points of 8L engine)

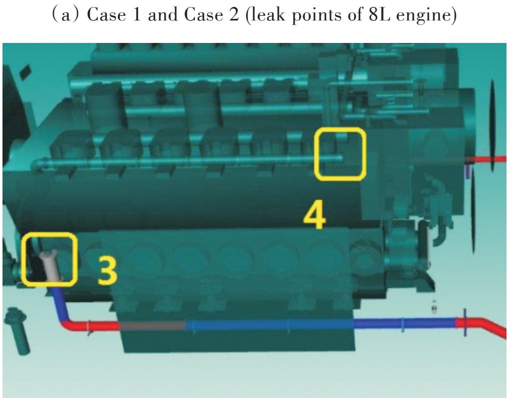

(b) Case 3 and Case 4 (leak points of 12V engine)

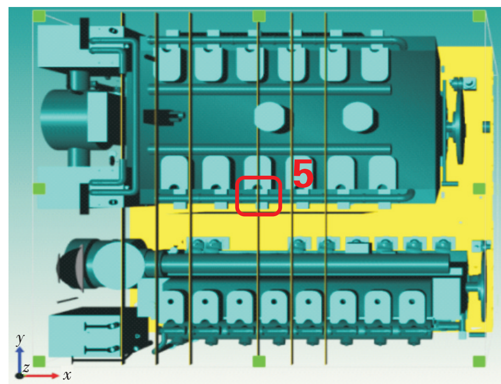

(c) Case 5 (leak point of 12V engine)

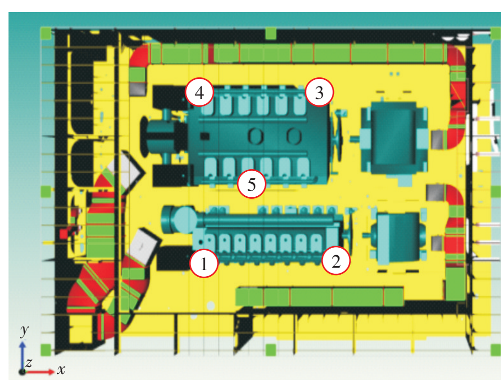

(d) Vertical view of locations of leak points

Fig.7 Locations of leak points

1.4.2 Leakage conditions

Pipeline damage leading to leakage is divided into entire damage and small-size damage. The entire damage of gas pipe results in rapid reduction of internal pressure to trigger fuel-gas differential-pressure alarm and shut down the fuel gas valve unit[22], and thus, it will not cause large-area leakage and long-time accumulation of fuel gas. By contrast, small-size damage is generally not enough to trigger the fuel-gas differential-pressure alarm, so it may incur continuous leak and accumulation of flammable gas. Natural gas is perceived difficultly because it is colorless and tasteless. Thus, flammable gas detectors are needed to give an alarm in advance. Therefore, the research object is small-size damage of gas pipe as the leakage condition.

The internal diameter and damage size of the pipe are set to be D and d respectively. When $d/D \leqslant 0.2$, small-size leakage model can be used for calculating the leak rate of gas. In the small-size leakage model, the pipe volume is regarded to be large enough, and it is assumed that the pressure in the pipe is not affected by leakage and remains constant[23]. The small-size leakage is regarded as an adiabatic process, and natural gas is regarded as ideal pure methane. Bernoulli equation and adiabatic equation are used, and the frictional loss during actual gas leakage is considered at the same time; then, the leak rate v_0 of gas is[24]

$$v_0 = \varphi \sqrt{\frac{2k}{k-1} RT[1-(\frac{p_0}{p_1})^{\frac{k-1}{k}}]} \tag{2}$$

where φ is the coefficient of flow rate at the orifice, i.e., the ratio of actual flow rate to theoretical flow rate, and it is generally set to be 0.97–0.98; p_1 is pressure in the gas pipe, Pa; p_0 is environmental pressure outside the pipe, Pa; k is adiabatic index and is generally set to be 1.3 for natural gas; R= 8.314 is molar gas constant, J(/mol·K); and T is gas temperature, K.

Supposing that the pressure in the pipe is 2.83×10^5 Pa (designed operation condition) and remains steady during leakage, the leak rate at the outlet is calculated to be 66.29 m/s according to Eq. (2). The internal diameter of gas pipe is set to be 102 mm, and the damage opening is a square opening with an area of 20 mm × 20 mm.

1.5 Solution and boundary condition settings

One exhaust fan is at the top of the engine room, and its ventilation system includes 3 air ducts and 21 air inlets. With respect to the inner space of the engine room, the air inlet of turbochargers of the two dual-fuel engines is also an exhaust outlet. The ambient pressure is set to be 101 325 Pa, and the wall surface is set to be adiabatic. The flow rate of gas at air inlet is 0.3 time smaller than sound velocity. Air and natural gas are regarded as incompressible ideal gases, and the inner flow field of the engine room is unsteady flow field. The boundary conditions are set as follows:

1) Inlet of air duct. For 21 air inlets, the inlet boundary of mass flow is used, and the mass flow (0.92–25.52 kg/s) is given according to the design parameters of actual ship. The inflow direction is vertical to the cross-section of inlet, and the ambient temperature is 300 K.

2) Outlet of exhaust fan at the top of the engine room. The boundary of the fan is used, and the mass flow is set to be 30.625 kg/s according to the operation conditions.

3) Exhaust outlet of turbocharger. The boundary of pressure outlet is used, and the outlet pressure is to be 0 Pa (gauge pressure).

Pressure-based coupled solver and implicit control equations are used for solving unsteady mass, momentum, energy and component transport equation, and pressure-velocity correlation adopts PISO format. In order to ensure precision, the second-order upwind scheme is used for numerical discretization of momentum, turbulent kinetic energy, and turbulent dissipation rate. During calculation, the convergence criterion of iterative residual volume is set to be 1×10^{-4} in continuity equation, 5×10^{-4} in component equation, and 1×10^{-3} in other control equations.

2 Calculation result and analysis

2.1 Ventilation calculation result

Because leakage of fuel gas in the engine room occurs under the ventilation condition, the time step is set to be 0.02 s for simulation calculation of unsteady ventilation flow field. The calculation result of ventilation flow field is regarded as the initial field of leakage and diffusion calculation. The specific gravity of natural gas is less than 1, and the natural gas will disperse upwards after leakage. Meanwhile, flammable gas detectors are arranged above the engine room. Thus, the horizontal z=8 m section is taken as the analysis cross-section, as shown in Fig. 8(a). Velocity vectors in this section at different moments are shown in Figs. 8(b)–8(h), where v_{max} =3.5 m/s.

As shown in Fig. 8, when t=1.2–5.2 s which is the initial stage of ventilation, the flow tendency in the section is not obvious and the flow rate in the main range of flow field is below 0.1 m/s. When t= 5.2–19.9 s, the velocity at each point increases and the flow rate in the main range reaches above 1 m/s. When t=19.9–51.3 s, the changes of local velocity and direction in the section are decreased. When t= 51.3–91.3 s, the flow rate and direction in the main range have shown no obvious changes and the flow field tends to be the same in the area with obvious flow tendency (the flow rate is more than 1 m/s); the difference is mainly centered on the area with weak

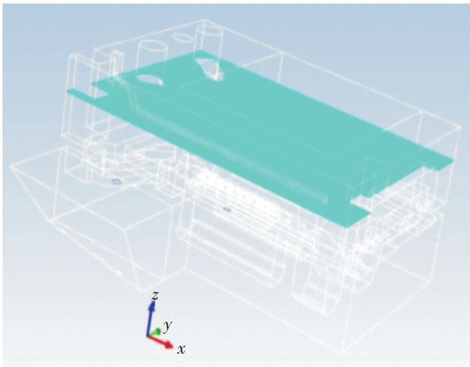

(a) z=8 m

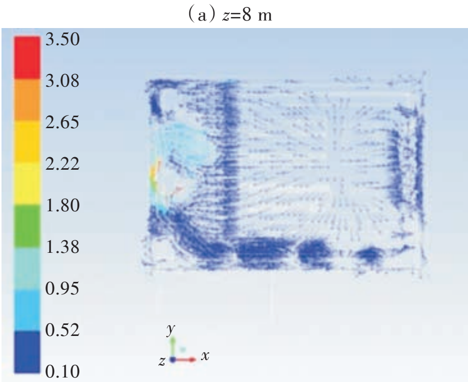

(b) t=1.2 s

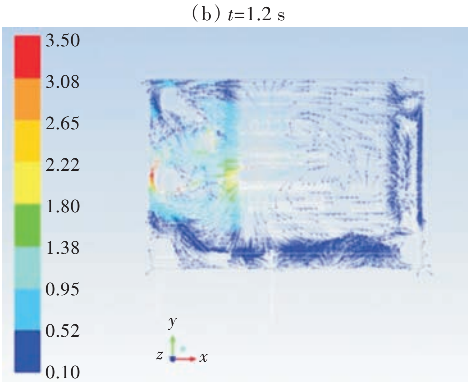

(c) t=5.2 s

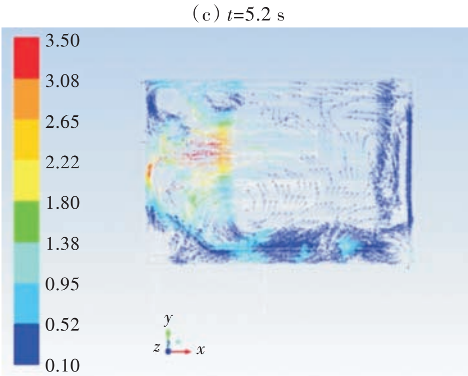

(d) t=10.2 s

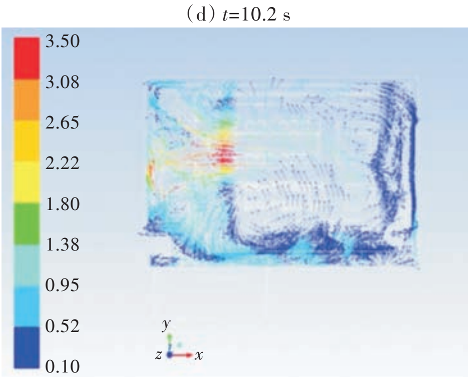

(e) t=19.9 s

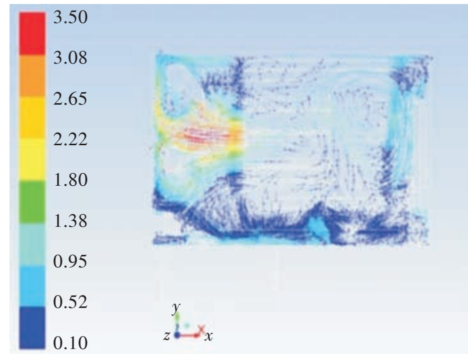

(f) t=51.3 s

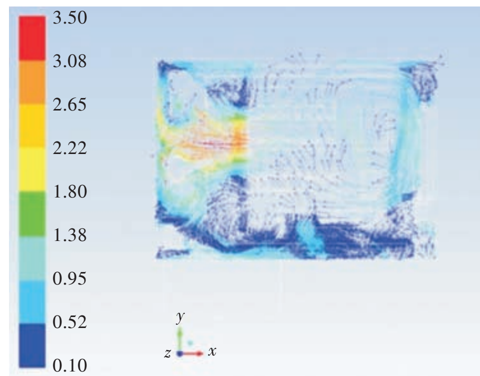

(g) t=71.3 s

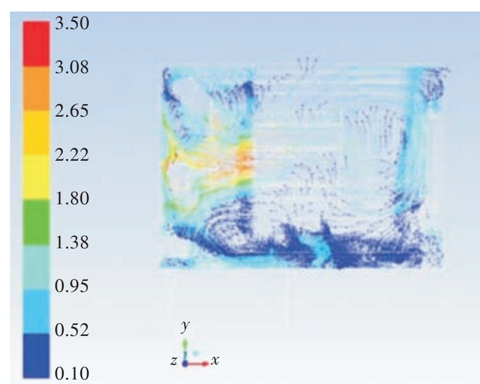

(h) t=91.3 s

Fig.8 Velocity vectors in z=8 m section at different times

flow (the flow rate is less than 0.5 m/s). Thus, the calculation result of the ventilation field at t=91.3 s is regarded as the initial field for calculation of leakage and diffusion.

In order to further analyze the flow field in the section, the main flow tendency of basically steady flow field (t=91.3 s) is marked with red arrows, as shown in Fig. 9. When $t \geqslant 51.3$ s, the main flow tendency in the section is similar to that in Fig. 9. In Fig. 9, the area marked by arrows 1 and 2 is just above the area 1 of fuel gas pipe shown in Fig. 4, and the overall flow is along $+x$ direction and then gradually turns to $-y$ direction after closing to the end; the area marked by arrow 3 is at the top of area 2 of fuel gas pipe, and the overall flow is along $-x$ direction. The flow direction at each point at the top of area 3 of fu-

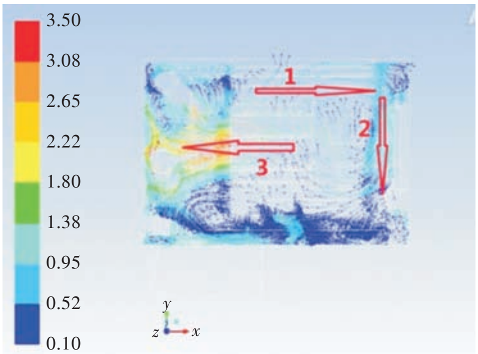

Fig.9 Main flow tendency in z=8 m section at t=91.3 s

el gas pipe is disperse in the flow field and has no obviously consistent flow direction; besides, it only presents a weak confluence tendency in $+y$ direction in the right area, and meanwhile, the overall flow rate at the top of area 3 is less than 1 m/s.

The analysis above shows the main flow tendency of gas after fuel gas leakage in different areas, but the velocity distribution in a single section is not enough to accurately determine the diffusion tendency of flammable gas after leakage. Besides influences of local wind speed and wind direction, the specific diffusion distribution is affected by jet speed, overall space flow, equipment blockage and poor density.

2.2 Calculation result of leakage and diffusion

2.2.1 Case 1

After natural gas leakage happens at Case 1, the molar concentration distribution of natural gas at different moments is shown in Fig. 10. Natural gas flows upwards under the effects of initial momentum and density difference, and diffuses all around under the additive effects of thermal motion of molecule and air flow turbulence. Thus, it is difficult to reach the top of the engine room. With the extension of time, the diffusion range is enlarged continuously, and the high concentration area of gas cloud is centered above the leakage opening.

2.2.2 Case 2

After natural gas leakage happens at Case 2, the molar concentration distribution of natural gas at different moments is shown in Fig. 11. Natural gas flows upwards and diffuses all around, which is similar to that at Case 1. However, natural gas has an obviously main flow direction, i.e., it mainly flows to the middle area of the engine room and diffuses all around after reaching the top. During the whole leakage, the high concentration area of gas cloud is centered in the middle of the engine room.

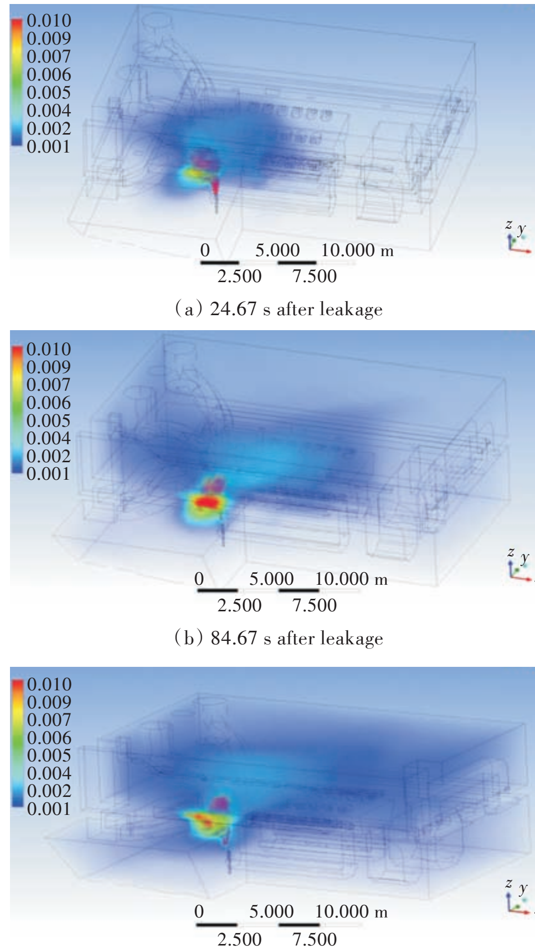

(a) 24.67 s after leakage

(b) 84.67 s after leakage

(c) 154.67 s after leakage

Fig.10 Distributions of natural gas mole concentration in engine room at different times for the continuous leak of Case 1

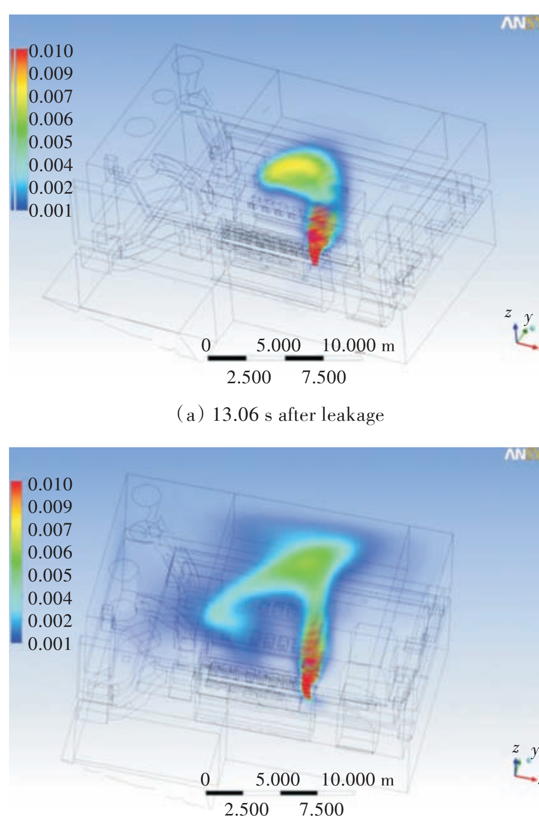

(a) 13.06 s after leakage

(b) 23.86 s after leakage

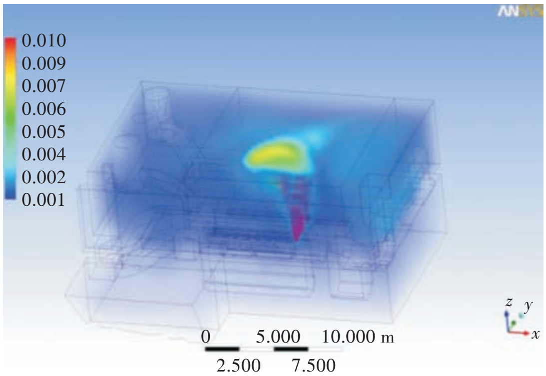

(c) 209.36 s after leakage

Fig.11 Distributions of natural gas mole concentration in engine room at different times for the continuous leak of Case 2

Both leak points of Case 1 and Case 2 are located in area 3 of fuel gas pipe (Fig. 4). With the combination of the flow tendency of ventilation field in z=8 m section (Fig. 9), it can be seen that: when leakage occurs in the left of area 3 (near Case 1), natural gas will diffuse all around in a short period of time and the high concentration area of gas cloud is centered above leak point; when leakage happens in the right of area 3 (near Case 2), natural gas will mainly flow to the middle of the engine room and the high concentration area of gas cloud is located in the middle-upper part of the engine room.

2.2.3 Case 3

After natural gas leakage happens at Case 3, the molar concentration distribution of natural gas at different moments is shown in Fig. 12. Natural gas mainly flows to the upper right part of the engine room (+x and +z directions) and diffuses along $-y$ direction after reaching the bulkhead, and the high concentration are of gas cloud is mainly located in the upper right of leak point.

2.2.4 Case 4

After natural gas leakage happens at Case 4, the molar concentration distribution of natural gas at different moments is shown in Fig. 13. Natural gas presents similar main flow tendency to that at Case 3, and it flows to the upper right part of the engine room and turns to $-y$ direction after reaching the bulkhead. The high concentration area of gas cloud is also mainly located in the upper right of leak point.

Both leak points of Case 3 and Case 4 are located in area 1 of fuel gas pipe (Fig. 4). With the combination of the flow tendency of ventilation filed in z=8 m section (Fig. 9), it can be seen that when leakage happens in area 1, natural gas will flow towards right with ventilation air flow and diffuse gradually, and the high concentration area of gas cloud is located in

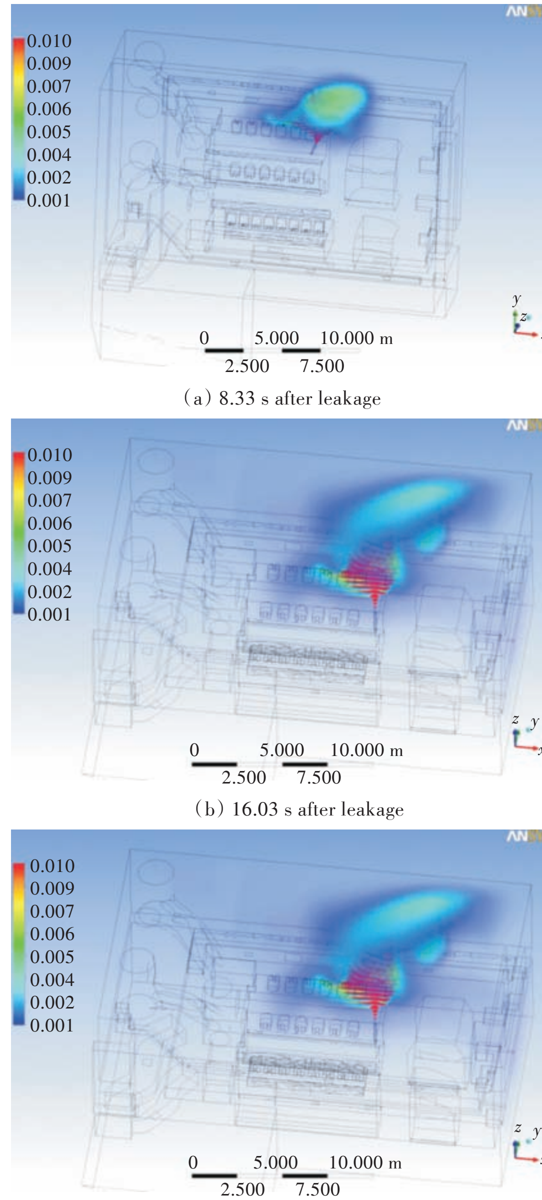

(a) 8.33 s after leakage

(b) 16.03 s after leakage

(c) 169.23 s after leakage

Fig.12 Distributions of natural gas mole concentration in engine room at different times for the continuous leak of Case 3

the upper right of leak point.

2.2.5 Case 5

After natural gas leakage happens at Case 5, the molar concentration distribution of natural gas at different moments is shown in Fig. 14. Natural gas mainly flows to the upper left ($-x$ and $+z$ directions), which is consistent with the flow tendency of ventilation field in z=8 m section. However, space hindrance of exhaust pipe will incur bypass flow. The total volume and height of gas cloud with molar concentration of greater than 0.1% in Case 5 are obviously less than those in cases 1-4. The reason is that the leak point of Case 5 is located in area 2 of fuel gas pipe where the ventilation effect is remarkably stronger than those in other areas (Fig. 9). In the

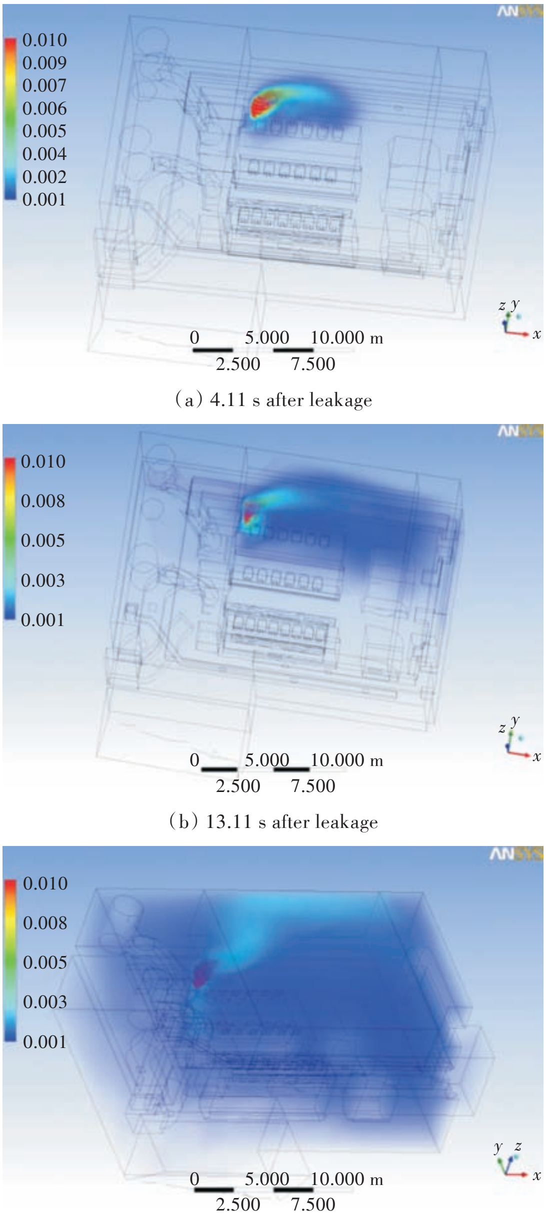

(a) 4.11 s after leakage

(b) 13.11 s after leakage

(c) 101.11 s after leakage

Fig.13 Distributions of natural gas mole concentration in engine room at different times for the continuous leak of Case 4

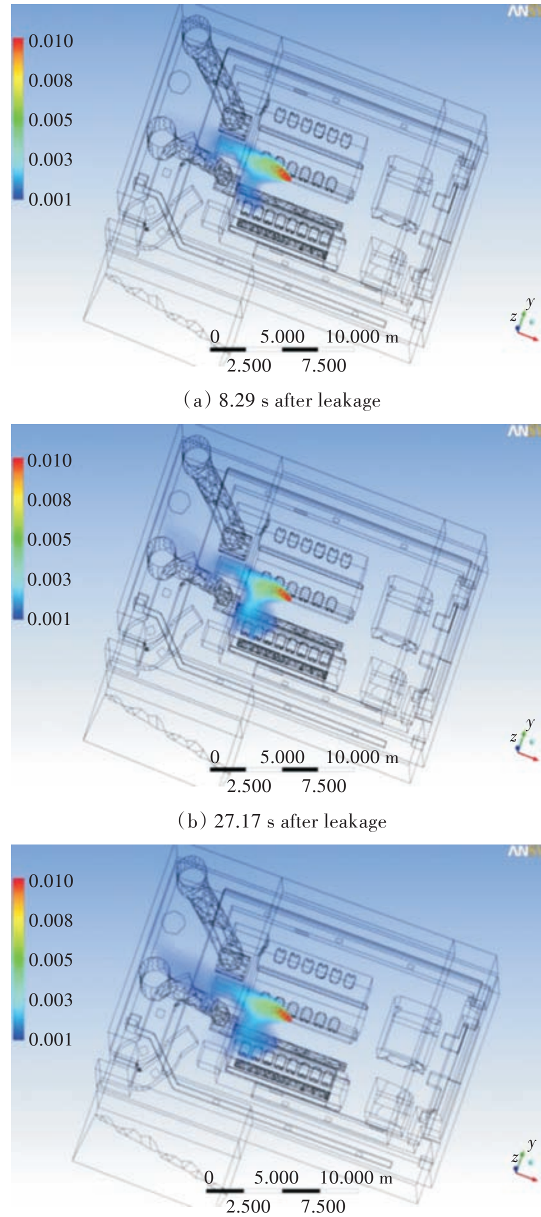

(a) 8.29 s after leakage

(b) 27.17 s after leakage

(c) 118.77 s after leakage

Fig.14 Distributions of natural gas mole concentration in engine room at different times for the continuous leak of Case 5

case, natural gas is blown away immediately after leakage and then discharged out by the exhaust fan in downwind direction, and thus, the concentration of gas cloud shows no obvious change within 8–118 s after leakage. After leakage occurs in this area, natural gas will mainly flow towards left ($-x$ direction) along the ventilation direction in the engine room and the high concentration area of gas cloud is located in the upper left of leak point.

2.3 Optimized arrangement of flammable gas detectors

In order to improve the detection precision, flammable gas detectors shall be arranged in the earliest high concentration area of gas cloud according to the diffusion tendency of natural gas. The main diffusion direction of leaked natural gas cloud in the engine room is principally affected by ventilation flow, but the gradient distribution of natural gas concentration still depends on concentration difference as driving force. Therefore, the high concentration area of gas cloud is generally located in the leeward side of leak point. By combining the characteristics of ventilation flow field with the diffusion tendency of natural gas in five typical cases, flammable gas detectors are arranged within 1 m from the top of the engine room, as shown in Fig. 15.

1) Area 1 of fuel gas pipe. After leakage of natural gas, the gas cloud mainly flows towards $+x$ direction and disperses very slowly. Thus, detectors 1 and 2

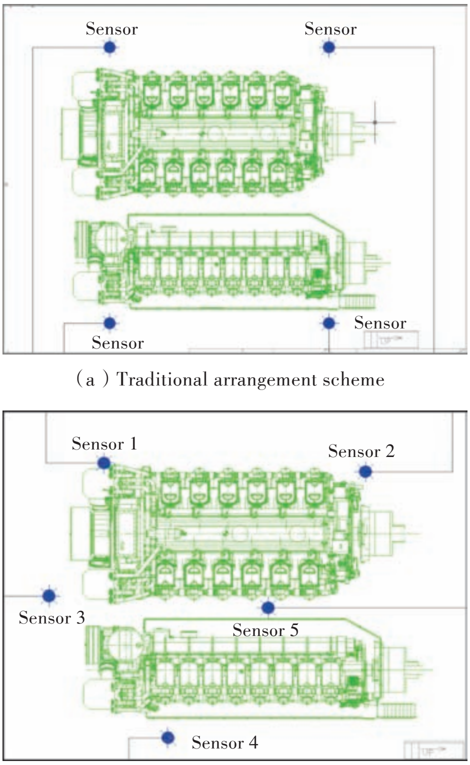

(a) Traditional arrangement scheme

(b) Computational analysis based arrangement scheme

Fig.15 Arrangement of flammable gas detectors

are arranged respectively in the middle and right end of area 1.

2) Area 2 of fuel gas pipe. After leakage of natural gas, the gas cloud chiefly presents an obvious flow tendency towards $-x$ direction and discharges from the exhaust fan at the top of the engine room. Therefore, detector 3 is arranged near the fan in area 2, while no detector is arranged in this area in traditional arrangement scheme. This area is in the leeward side of strong ventilation and close to the exhaust fan, and it is generally in the diffusion area of gas after leakage.

3) Area 3 of fuel gas pipe. There is relatively independent weak vortex flow in the upper left of the engine room. Thus, the gas cloud after leakage in this location gathers above the leak point and diffuses all around, while the gas cloud after leakage in the right flows towards the middle of the engine room. Therefore, detectors 4 and 5 are arranged respectively in the left of area 3 and in the middle of the engine room, while there is no detector in these areas in traditional arrangement scheme.

2.4 Demand evaluation of explosion-proof exhaust fan

With the increase of explosion-proof class of equipment, the procurement and maintenance fees also increase by times. The simulation results of leakage and diffusion can provide qualitative and quantitative assessment basis for explosion-proof class of equipment and classification of hazardous areas, so as to eliminate the potential risk or avoid unnecessary resource waste.

In this paper, exhaust fan at the top of the engine room is taken for example (Fig. 5(a)). It can be seen through the simulation results of leakage and diffusion that the concentration of accumulative natural gas near the fan is still far less than the lower explosive limit of natural gas (the molar concentration is 4.9%, and the upper explosive limit of natural gas is molar concentration of 9.5%) under dangerous leak conditions. According to optimized arrangement of flammable gas detectors, even if there is longstanding continuous leak accumulation, the area where the concentration is the earliest close to the lower explosive limit is also located near detectors which will give an alarm and cut off fuel gas in time. In the case that the concentration of natural gas near exhaust fan is always lower than the lower explosive limit of natural gas, even if equipment breaks down, it will not generate fire or explosion. Therefore, the adoption of an explosion-proof exhaust fan is proven to be unnecessary in the engine room.

3 Conclusions

In this paper, three-dimensional calculation model of the engine room is established. Firstly, the characteristics of unsteady ventilation flow field in the engine room are analyzed. Then, the leakage and diffusion of fuel gas pipe are simulated in different areas, thereby obtaining the diffusion tendency of natural gas and the location of high concentration gas cloud in different areas after leakage. Finally, the optimized arrangement scheme of flammable gas detectors is proposed. This provides quantitative basis for demand evaluation of explosion-proof exhaust fan, and also reference for prevention of leak accidents and improvement of the design. In the future, the characteristics of ventilation flow field will be further analyzed so as to optimize the arrangement of air duct and the distribution of air volume, thereby achieving consumption reduction and efficiency improvement; the burning explosion risk and load will be calculated and used for local reinforcement design of support structure.

References

[1] WEI L, GENG P. A review on natural gas/diesel dual fuel combustion, emissions and performance[J]. Fuel

Processing Technology, 2016, 142: 264-278.

[2] KUMAR S, KWON H T, CHOI K H, et al. LNG: an eco-friendly cryogenic fuel for sustainable development [J]. Applied Energy, 2011, 88(12): 4264-4273.

[3] LIN W, ZHANG N, GU A. LNG (liquefied natural gas): a necessary part in China's future energy infrastructure[J]. Energy, 2010, 35(11): 4383-4391.

[4] THOMSON H, CORBETT J J, WINEBRAKE J J. Natural gas as a marine fuel[J]. Energy Policy, 2015, 87: 153-167.

[5] SUN P T. "十二五"期间航运业和造船业热点与难点问题 [J]. World Shipping, 2013, 36 (1): 1-8 (in Chinese).

[6] ZHANG M F, DENG K. Introduction of LNG fuel ship's present situation[J]. Energy Research and Management, 2013(3): 16-20 (in Chinese).

[7] KUMAR S, KWON H T, CHOI K H, et al. Current status and future projections of LNG demand and supplies: a global prospective[J]. Energy Policy, 2011, 39(7): 4097-4104.

[8] ZHAO X W, YU L, CHAI J S. 天然气管道安全 [M]. Beijing: Chemical Industry Press, 2013 (in Chinese).

[9] FANG D X. Discussion on the analysis and its countermeasure of the elements on NG pipeline's security harmful[J]. Shanghai Gas, 2008(3): 38-41(in Chinese).

[10] OHBA R, KOUCHI A, HARA T, et al. Validation of heavy and light gas dispersion models for the safety analysis of LNG tank [J]. Journal of Loss Prevention in the Process Industries, 2004, 17(5):325-337.

[11] HUANG Q, JIANG J C. Simulation and verification of CFD on the dispersion of heavy gas leakage [J]. China Safety Science Journal, 2008, 18(1): 50-55 (in Chinese).

[12] DNV G L. Dual fuel concept analysis of fires and explosions in engine room [R]. Norway: DNV G L, 2006.

[13] CHENG H L, LIU D J, LIU Q Q, et al. CFD modeling of the releases and dispersion of accidental city gas pipeline in urban street canyons [J]. Journal of Petrochemical Universities, 2011, 24 (4): 60-63 (in Chinese).

[14] WANG L H. Study on the diffusion simulation of leaked oilgas on offshore platforms based on CFD [D]. Qingdao: Ocean University of China, 2014 (in Chinese).

[15] FU S S, YAN X P, ZHANG D, et al. Framework for the quantitative assessment of the risk of leakage from LNG-fueled vessels by anevent tree-CFD[J]. Journal of Loss Prevention in the Process Industries, 2016, 43: 42-52.

[16] FIATES J, SANTOS R R C, NETO F F, et al. An alternative CFD tool for gas dispersion modelling of heavy gas[J]. Journal of Loss Prevention in the Process Industries, 2016, 44: 583-593.

[17] IMO. Quantitative risk assessment of a fuel preparation room having a high-pressure fuel gas supply system on an LNG-fuelled ship[R]. Korea: Sub-Committee on Carriage of Cargoes and Containers, 2016.

[18] VERSTEEG H K, MALALASEKERA W. An introduction to computational fluid dynamics: the finite volume method[M]. [s.l.]Longman, 1996.

[19] Ansys Inc. Ansys fluent theory guide release 13.0[Z]. Ansys Inc, 2010: 67-78.

[20] CEHLIN M, MOSHFEGH B. Numerical modeling of a complex diffuser in a room with displacement ventilation [J]. Building and Environment, 2010, 45 (10): 2240-2252.

[21] GUO D P, YAO R T, QIAO Q D. Numerical and wind-tunnel simulation on the effect of building on pollutant dispersion [J]. Journal of Experiments in Fluid Mechanics, 2010, 24(6): 16-21 (in Chinese).

[22] MAN Diesel and Turbo. Safety concept dual-fuel engines[R]. Germany: MAN Diesel and Turbo, 2012: 12-20.

[23] WANG X. Hazard assessment of natural gas pipeline leakage and diffusion [D]. Harbin: Harbin Institute of Technology, 2010 (in Chinese).

[24] LI Y L, YAO A L, LI Y J. Study on diffusion model of gas pipeline leaking[J]. Natural Gas Industry, 2004, 24(8): 102-104 (in Chinese).

大型LNG船发电机室的燃气管线泄漏分析

岑卓伦，刘涛，王磊，窦旭

沪东中华造船(集团)有限公司 开发所，上海 200129

摘　要：[**目的**] 目前，由双燃料发动机组成的电力推进系统是大型液化天然气(LNG)船的主流推进方式，必须对爆炸性可燃气体进行安全可靠性的定性、定量评估，以规避潜在风险。[**方法**] 以某双燃料电力推进大型LNG船发电机室为研究对象，对其内部不同区域的燃气(天然气)泄漏工况进行模拟分析。根据泄漏发生的形式、位置和速率等定义危险泄漏工况，选择雷诺应力模型为湍流模型，采用计算流体力学(CFD)软件Fluent对发电机室燃气供应管线的5个泄漏点进行持续泄漏模拟计算，并将泄漏扩散结果与舱室通风的流场速度分布相结合，得到不同区域发生泄漏后的天然气扩散趋势和浓度分布。[**结果**] 根据仿真模拟结果优化了可燃气体探测器布置方案，并明确了排气风机无需进行防爆设计。[**结论**] 研究结果可为有限空间内通风条件下的可燃气体泄漏事故分析防范提供参考，并且适用于燃烧爆炸破坏的定量评估，用以指导结构强度设计。

关键词：液化天然气；管道泄漏；计算流体力学；定量风险评估